

A Design and Rating Method for Shell-and-Tube Heat Exchangers With Helical Baffles

Jian-Fei Zhang

Ya-Ling He

Wen-Quan Tao¹

e-mail: wqtao@mail.xjtu.edu.cn

School of Power and Energy Engineering,
Xi'an Jiaotong University,
Xi'an 710049, China

A method for design and rating of shell-and-tube heat exchanger with helical baffles (STHXHB) has been developed in present study based on the public literatures and the widely used Bell–Delaware method for shell-and-tube heat exchanger with segmental baffles (STHXsSB). A number of curve-type factors in the literature have all been replaced by mathematical expressions for the convenience of engineering design. The detailed calculation procedure of the method is provided. The accuracy of present method is validated with some experimental data. Four design cases of replacing original STHXsSB by STHXsHB are supplied, and the comparison results show that all of the STHXsHB have better performance than the original heat exchangers with segmental baffles.

[DOI: 10.1115/1.4000457]

Keywords: shell-and-tube heat exchanger, helical baffle, pressure drop, heat transfer, design and rating method

1 Introduction

Shell-and-tube heat exchangers (STHXs) are widely used in many industrial areas, and more than 35–40% of heat exchangers are of this type due to their robust geometry construction, easy maintenance, and possible upgrades [1]. Besides supporting the tube bundles, the baffles in shell-and-tube heat exchangers form flow passage for the shell-side fluid in conjunction with the shell. The most-commonly used baffle is the segmental baffle, which forces the shell-side fluid going through in a zigzag manner, hence, improves the heat transfer with a large pressure drop penalty. This type of heat exchanger has been well-developed [2–6] and probably is still the most-commonly used type of the shell-and-tube heat exchangers. But there are three major drawbacks in the conventional shell-and-tube heat exchangers with segmental baffles (STHXsSB): (1) the large shell-side fluid pressure drop; (2) the dead zone in each compartment between two adjacent segmental baffles, which lead to an increase of fouling resistance; and (3) the dramatic zigzag flow pattern and longer unsupported tube spans, which lead to high risk of vibration failure of tube bundle. A number of improved structures were proposed for the purposes of higher heat transfer coefficient, low possibility of tube vibration, and reduced fouling factor with a mild increase in pumping power [7–11].

However, the principal shortcomings of the conventional segmental baffle still remain in the improved structures of the above-mentioned studies. A new type of baffle, called the helical baffle, provides further improvement. This type of baffle was first developed by Lutchka and Nemcansky [12]. They investigated the flow field patterns produced by such helical baffle geometry with different helix angles. They found that these flow patterns were very close to the plug flow condition, which was expected to reduce shell-side pressure drop and to improve heat transfer performance. Stehlik et al. [13] compared heat transfer and pressure drop correction factors for a heat exchanger with an optimized segmental baffle based on the Bell–Delaware method [2–4] with those for a heat exchanger with helical baffles. Kral et al. [14] discussed the performance of heat exchangers with helical baffles based on test

results of various baffles geometries. One of the most important geometric factors of the STHXHB is the helix angle. Recently a comprehensive comparison between the test data of shell-side heat transfer coefficient versus shell-side pressure drop was provided for five helical baffles and one segmental baffle measured for oil-water heat exchanger [15]. It is found that based on the heat transfer per unit shell-side fluid pumping power or unit shell-side fluid pressured drop, the case of 40 deg helix angle behaves the best.

For the convenience of manufacturing, up to now all helical baffles actually used in STHXs are noncontinuous approximate helicoids. The noncontinuous helical baffles are usually made by four elliptical sector-shaped plates joined in succession. The elliptical sector-shaped plates are arranged in a pseudohelical (noncontinuous) manner, with each baffle occupying one-quarter of the cross section of the heat exchanger and being angled to the axis of the heat exchanger. The two adjacent baffles may be joined end to end at the perimeter of each sector, forming a continuous helix at the outer periphery (Fig. 1(a)); this structure of connecting baffles together is called a single helix manner. Another connection between two adjacent sectors is the middle-overlapped connection, as shown in Fig. 1(b), where the helix angle, designated by β , helical pitch, B , and baffle thickness, S_p , are presented. As shown in Fig. 1(c), the helix angle is referred to as the angle between the normal line of the elliptical sector-shaped plates and the heat exchanger axis. For heat exchangers with large shell diameters, such structures can reduce the helical pitch to shorten the length of heat exchanger and can also reduce the cross-flow area to obtain a higher shell-side velocity. Hence such connection is more popular in engineering practice. Typical publications on experimental study of STHXsHB since the year 2000 can be referred to in Refs. [15–19]. With the rapid advances in computer hardware numerical simulation plays an increasingly important role. Typical progresses in the shell-and-tube heat exchanger performance simulations can be found in Refs. [20–39].

The research results of experimental measurements and numerical simulations provide the bases of engineering design method, for which the primary objects are to determine the required heat transfer surfaces and the fluid pressure drops of shell-and-tube sides. In the design method, the input data are flow rates and at least three of the inlet and outlet temperatures of both sides in heat exchanger. After primary guessing for the heat exchanger structure, the over-all heat transfer coefficient and the pressure drop

¹Corresponding author.

Contributed by the Heat Transfer Division of ASME for publication in the JOURNAL OF HEAT TRANSFER. Manuscript received May 7, 2009; final manuscript received August 23, 2009; published online March 9, 2010. Assoc. Editor: G. Lorenzini.

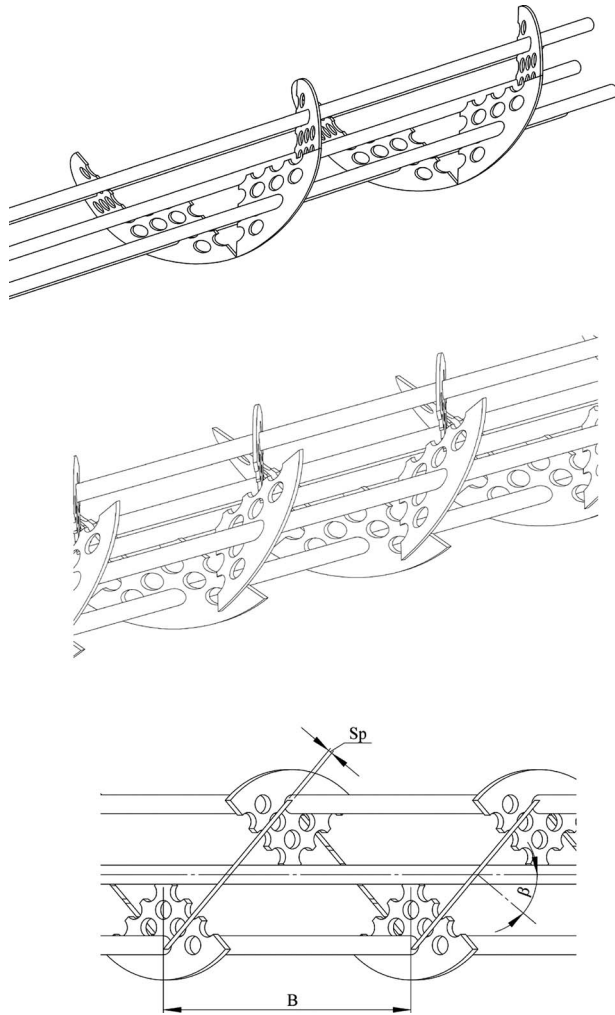


Fig. 1 Helical baffle arrangement and parameters definition

can be determined by adopting correlations obtained from tests or simulations. If the calculated heat transfer rate and pressure drops cannot satisfy the design requirements, the heat exchanger is reconstructed, and the calculation is repeated again until the calculated heat transfer rate and the pressure drops can satisfy the pre-specified conditions. It can be seen that the heat transfer and pressure drop correlations are the basis for the design method.

The above-mentioned engineering design method has been quite well-developed for the conventional segmental baffled shell-and-tube heat exchangers (STHXsSB) [2–6,11,40–51]. However, for STHXsHB, the situation is totally different. Except the early work published by Stehlik et al., we can hardly find papers related to the design method of STHXsHB. Reference [37] is the only one known to the present authors. In Ref. [13] a comprehensive comparison was made for the flow and heat transfer characteristics of STHXsSB and STHXsHB, and based on the design method for the STHXsSB, a series of correction curves were provided for the calculation of pressure drop and heat transfer coefficient of STHXsHB. But, the complete design method and procedure for determination of geometry parameters of both sides in STHXsHB were not provided in Ref. [13]. Of course this is not convenient to the engineering application. In Ref. [37], part of the design methods is based on the results in Ref. [13], but the detailed design procedure and the determination of geometry parameters of both sides in STHXsHB were not supplied either. This situation is obviously not convenient for a good engineering design of a STHXHB.

Stimulated by the above-mentioned situation, in this paper the present authors propose a complete calculating method for the design of a STHXHB in detail via a number of equations based on the study results in Ref. [13] and the Bell–Delaware method [2–6]. The accuracy of this method is validated by comparison with the experiment data in Ref. [15]. Finally, some application cases of this method are presented.

2 Correlations for Flow and Heat Transfer Characteristics in Shell Side of STHXsHB

Based on Refs. [2–6,13] the correlations for flow and heat transfer in shell side of STHXsHB are proposed and collected in this section. Most of the symbols used the following presentation are the same as what were used in Ref. [13] for the sake of convenience.

2.1 Correlations for Heat Transfer Coefficient in Shell Side of STHXsHB. The average Nu number for the shell side of STHXsHB [13] is determined by

$$\text{Nu}_s = 0.62 \times (0.3 + \sqrt{\text{Nu}_{\text{lam}}^2 + \text{Nu}_{\text{turb}}^2}) \times Y_2 \times Y_3 \times Y_4 \times Y_7 \times Y_8 \times Y_9 \times Y_{10} \quad (1)$$

where

$$\text{Nu}_{\text{lam}} = 0.664 \text{Re}^{0.5} \text{Pr}^{0.33} \quad (2)$$

$$\text{Nu}_{\text{turb}} = \frac{0.037 \text{Re}^{0.7} \text{Pr}}{1 + 2.433 \text{Re}^{-0.1} (\text{Pr}^{0.67} - 1)} \quad (3)$$

In Eq. (1) coefficients Y_i are the correction factors. Their physical meanings are defined as follows [13]. Y_2 accounts for the thermal-physics properties effects; Y_3 accounts for the scale-up from a single tube row to a bundle of tubes; Y_4 accounts for the adverse temperature gradient; Y_7 accounts for the bundle-shell bypass streams; Y_8 accounts for the baffle spacing in inlet and outlet sections; Y_9 accounts for the change in the cross-flow characteristics in heat exchanger; and Y_{10} accounts for the turbulent enhancement.

Average heat transfer coefficient for shell side of STHXsHB [13] is

$$h_s = \frac{\text{Nu}_s \times \lambda_s}{l} \quad (4)$$

where

$$l = \frac{\pi d_o}{2} \quad (5)$$

where d_o is the outside diameter of the tube; and λ_s is thermal conductivity of shell-side fluid. The application ranges of Eqs. (1)–(5) are $10 < \text{Re} < 10^6$, $10 < \text{Pr} < 10^3$, $n_{rc} > 10$, and $5 \leq \beta \leq 45$ deg, where

$$n_{rc} = n_{rp}(n_p - 1) \quad (6)$$

n_{rp} is the number of tube rows in the cross section of heat exchanger; and n_p is the number of baffles.

2.2 Correlations for Pressure Drop in Shell Side of STHXsHB. According to Stehlik et al. [13], the pressure drop cross the bundle per unit cycle without bypass flow can be determined by

$$\Delta p_{f0}^1 = 2\lambda_{22} n_r^1 \rho_2 u_2^2 Z_2 Z_6 Z_7 \quad (7)$$

The pressure drop cross the whole bundle zone with bypass flow is [13]

$$\Delta p_{f0} = \Delta p_{f0}^1 \frac{l_0}{B} Z_3 \quad (8)$$

The pressure drop in the inlet and outlet zones [13]

$$\Delta p_{in} = \Delta p_{t0}^1 Z_5 \quad (9)$$

where n_r^1 is the number of tube rows on the center stream line within one cycle. λ_{22} is the friction factor of ideal cross-flow through tube bundle, which can be determined by referring to [6,52]. l_{t0} is the baffled length of tube bundle.

In Eqs. (7)–(9) correction factors are defined as [13] follows. Z_2 accounts for the thermal-physics properties effects; Z_3 accounts for the bundle-shell bypass streams; Z_5 accounts for the baffle spacing in inlet and outlet sections; Z_6 accounts for the change in the cross-flow characteristics in heat exchanger; and Z_7 accounts for the turbulent enhancement.

The pressure drop in the inlet and outlet nozzles can be calculated by [53,54]

$$\Delta p_{nozzle} = \xi \times 0.5 \times \rho v_{s,nozzle}^2 \quad (10)$$

where ξ is taken as 1.5 or 2.0 by referring to Refs. [53,54].

The over-all pressure drop of the shell-side fluid

$$\Delta p_{s,all} = \Delta p_{in} + \Delta p_{nozzle} + \Delta p_{t0} \quad (11)$$

From above presentation it can be seen that the determination of factors Y_i and Z_i is the key issue to obtain the shell-side fluid heat transfer coefficient and pressure drop. Section 2.3 is for this purpose.

2.3 Determination of Factors. Y_2 and Z_2 [6,13].

$$Y_2 = \left(\frac{\eta_s}{\eta_{s,w}} \right)^{0.14} \quad (12)$$

$$Z_2 = \left(\frac{\eta_s}{\eta_{s,w}} \right)^{-0.14} \quad (13)$$

where $\eta_{s,w}$ is the dynamic viscosity at average temperature of tube wall.

The determination of average temperature of tube wall is conducted by [6]

$$t_w = t_{t,avg} + \left(\frac{t_{s,avg} - t_{t,avg}}{1 + h_t/h_s} \right) \quad (14)$$

where $t_{t,avg}$ and $t_{s,avg}$ are the averaged inlet and outlet temperatures of tube side and shell side in the heat exchanger, respectively. h_t and h_s are heat transfer coefficients for tube side and shell side, respectively.

Y_3 [13,52]. For in-line arrangement,

$$Y_3 = 1 + \frac{0.7}{\varepsilon^{1.5}} \frac{b/a - 0.3}{(b/a + 0.7)^2} \quad (15)$$

For staggered arrangement,

$$Y_3 = 1 + \frac{2}{3b} \quad (16)$$

where a is the ratio of distance between the tube normal to the flow direction and the central tube pitch, b , is the ratio of distance between tube in the flow direction and the central tube pitch, as shown in Fig. 2, and the parameter ε is determined by

$$\text{if } b \geq 1: \quad \varepsilon = 1 - \frac{\pi}{4a} \quad (17)$$

$$\text{if } b < 1: \quad \varepsilon = 1 - \frac{\pi}{4ab} \quad (18)$$

Y_7 and Z_3 [13]. Y_7 and Z_3 are functions of $t_t \cdot n_{pt}/D_1$ and S_{ss}/S_{2z} , as shown in graphs presented by Stehlik et al. [13]. These curves have been fitted to the following equations (using x and y , respectively, to substitute $t_t \cdot n_{pt}/D_1$ and S_{ss}/S_{2z} for simplicity):

$$Y_7 = \exp[-1.343x(1 - (2y)^{0.338})] \quad (19)$$

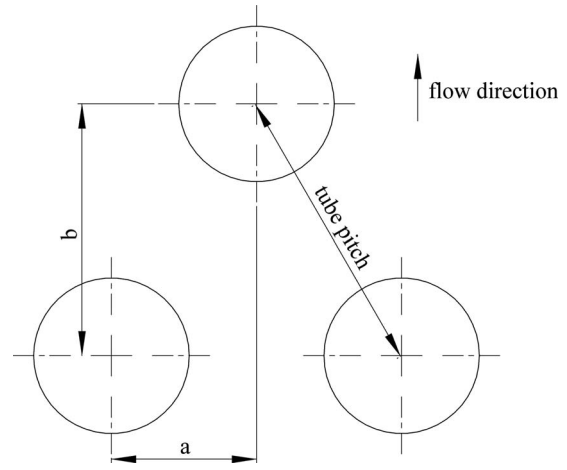


Fig. 2 Definition of parameters used in Y_3

$$Z_3 = \exp[-3.56x(1 - (2y)^{0.363})] \quad (20)$$

where

$$S_{ss} = 0.5(B - S_p/\cos \beta)[D_1 - D_s - S_{tt}] \quad (21)$$

$$S_{2z} = 0.5(B - S_p/\cos \beta) \left[D_i - D_1 + \frac{D_1 - d_o}{t_t}(t_t - d_o) \right] \quad (22)$$

In the above equations, t_t is the tube pitch, D_1 is the inner diameter of shell, S_p is the thickness of baffle, S_{tt} is distance between the two tubes' outside surfaces, n_{pt} is the number of stealing strip pairs, and D_s is the diameter of tube bundle. It should be emphasized that for the STHXsHB because the shell-side flow pattern resulted from the helical-type structure is close to helical flow, the cross section area, S_{2z} , is actually only half of the entire cross section at the shell centerline of the heat exchanger.

Y_8 and Z_5 [13]. Y_8 and Z_5 are functions of $(l_{tc} - l_{t0})/l_{tc}$ and B/D_1 , as shown in graphs presented by Stehlik et al. [13]. Again, the present authors have made curve-fitting for the convenience of design as follows (using x and y , respectively, to substitute $(l_{tc} - l_{t0})/l_{tc}$ and B/D_1 for simplicity):

$$Y_8 = 1.079y^{0.0487} - 0.445y^{-0.301}x^{1.2} \quad (23)$$

$$Z_5 = (-0.0172 + 0.0899y)x^{-1.2} \quad (24)$$

where l_{tc} is the effective length of the tube bundle, and l_{t0} is the baffled length of tube bundle.

Figure 3 illustrates the definitions of l_{t0} and l_{tc} . The helical pitch B can be calculated with D_1 and β at hand (see Eq. (25)) [55], and then the maximum number of baffle numbers can be determined

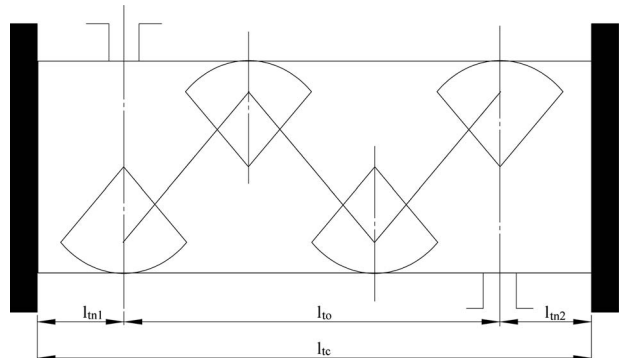


Fig. 3 Definition of parameters used in Y_8 and Z_5

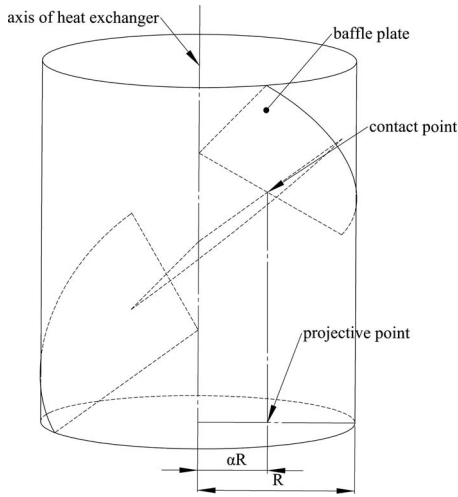


Fig. 4 Definition of overlapped rate α

with specified value of l_{tc} . The baffle number is an integral. Then l_{t0} and the distances between inlet and outlet baffles to tube sheet, l_{m1} and l_{m2} , can be determined with ease

$$B = \alpha n \cdot D_1 \sin \frac{\pi}{n} \cdot \tan \beta, \quad n \geq 2, \quad 0 < \alpha \leq 1 \quad (25)$$

where α is the dimensionless radius of the contacting point of the two successive helical baffles (see Fig. 4).

Y_9 and Z_6 [13]. From the graphs presented by Stehlik et al. [13], Y_9 and Z_6 are only influenced by helical angle. The curves in [13] can be fitted to the following equations:

$$Y_9 = 0.977 + 0.00455x - 0.0001821x^2 \quad (18 \text{ deg} \leq x \leq 45 \text{ deg}) \quad (26)$$

$$Y_9 = 1 \quad (x < 18 \text{ deg}) \quad (27)$$

$$Z_6 = 0.289 - (5.06 \times 10^{-4})x - (4.53 \times 10^{-5})x^2 \quad (28)$$

where x represents the helical angle β .

Y_{10} and Z_7 [13]. Y_{10} and Z_7 are also only influenced by the helical angle, as shown in the graphs presented by Stehlik et al. [13]. The following curve-fitted equations are obtained by the present authors:

$$Y_{10} = -56.39 + 8.28x - 0.46x^2 + 0.012x^3 - (1.64 \times 10^{-4})x^4 + (8.19 \times 10^{-7})x^5 \quad (25 \text{ deg} < x < 45 \text{ deg}) \quad (29)$$

$$Y_{10} = 1 \quad (x < 25 \text{ deg}) \quad (30)$$

$$Z_7 = -5.411 + 0.379x - 0.00402x^2 \quad (22 \text{ deg} < x < 45 \text{ deg}) \quad (31)$$

$$Z_7 = 1 \quad (x < 22 \text{ deg}) \quad (32)$$

where x represents the helical angle β .

3 Correlations for the Flow and Heat Transfer in Tube Side of STHXsHB

3.1 Correlations for Heat Transfer Coefficient in Tube Side of STHXsHB. The average heat transfer coefficient of tube side is calculated by the Gnielinski equation in turbulence condition or the Sieder–Tate equation in laminar condition [56–58].

3.2 Correlations for Pressure Drop in Tube Side of STHXsHB [53,54].

$$\Delta p_{t,\text{all}} = \frac{1}{2} \xi \rho v_{t,\text{nozzle}}^2 + \frac{1}{2} \rho v_t^2 \left[\frac{f_t L_{tc}}{d_i} \frac{1}{(\phi_t)^r} + k_c + k_e + 4 \right] N_p \quad (33)$$

where ξ is taken as 1.5 or 2.0 [53,54]; k_c and k_e are friction factors for the sudden contraction and expansion effects, respectively, when the tube side fluid flows into and out of the tubes; N_p is the number of tube passes; and if there is only one tube pass in the heat exchanger, the number “4” in Eq. (33) should be omitted. The friction factor f_t can be determined by referring to Refs. [53,54].

4 Design Procedures

In heat transfer textbooks heat exchanger design is often classified by the design mode and rating mode [54,56,57]. Simply speaking, in the design mode the heat transfer rate is given and the required heat transfer surface area is searched for, while the rating mode is applied for an existing heat exchanger to find its capability of heat transfer at some given condition. The present design method can be used for both design mode and rating mode. For the convenience of presentation the procedure of the design mode is first presented in detail. For the design mode the task is to determine all the geometry parameters of one heat exchanger, which can satisfy the request heat duty and maximum allowable pressure drop.

Procedure for design mode is listed as follows:

- (1) Define the heat duty of each side by Eqs. (34) and (35), respectively

$$\Phi_s = M_s \times c_{ps} \times |t_{s,\text{in}} - t_{s,\text{out}}| \quad (34)$$

$$\Phi_t = M_t \times c_{pt} \times |t_{t,\text{in}} - t_{t,\text{out}}| \quad (35)$$

The deviation between the heat duties of both sides, Φ_s and Φ_t , should be lower than 5% for a conventional engineering design.

- (2) Determine the tube layout pattern such as 30 deg, 45 deg, and 90 deg layout pattern.
- (3) Determine the thermophysical properties of the tube side and shell-side fluids at its reference temperature, which is usually taken as the average magnitude of the inlet and outlet temperatures of corresponding sides.
- (4) Guess the primary over-all heat transfer coefficient K_0 and calculate the primary requested heat transfer area A_o by Eq. (36), and Δt_m is the logarithmic mean temperature difference

$$A_o = \frac{\Phi_s}{K_0 \cdot \Delta t_m} \quad (36)$$

- (5) Fix the tube effective length or the inner diameter of the shell; if the tube effective length is fixed, the tube number can be determined by Eq. (37)

$$A_o = N_t \cdot \pi d_o l_{tc} \quad (37)$$

and the diameter of tube bundle can be carried out by referring to graphs or empirical formula in Ref. [6]. Then the inner diameter of shell can be defined based on the diameter of tube bundle.

If the inner diameter of shell is fixed, the diameter of tube bundle can be defined at first, and the tube number also can be determined by referring to graphs or empirical in Ref. [6].

- (6) Choose the helical angle and overlap ratio of helical baffles.
- (7) Calculate the shell-side velocity and tube side velocity, determine the Re number of each side, then calculate the value of correction factors according to the discussion in Sec. 2.3.
- (8) Carry out the heat transfer coefficient and pressure drop for each side under present geometry and obtain the over-all heat transfer coefficient by Eq. (36)

Table 1 Helical baffled shell-and-tube heat exchanger geometry

Item		Dimensions and description		
Shell-side parameters	D_o/D_i /mm	325/313	325/313	223/211
	Material	0Cr18Ni9	0Cr18Ni9	0Cr18Ni9
Tube parameters	d_o/d_i /mm	19/15	19/15	19/15
	Effective length/mm	1194	1608	1703
	No.	97	97	37
	Layout pattern	45 deg	45 deg	45 deg
	Tube pitch/mm	25	25	25
Baffle parameters	Material	0Cr18Ni9	0Cr18Ni9	0Cr18Ni9
	Baffle pitch/mm	161	255	250
	Helix angle	20 deg	30 deg	40 deg
	Thickness/mm	3	3	3
	No.	24	24	24

$$\frac{1}{k} = \frac{1}{h_i} \frac{d_o}{d_i} + \frac{d_o}{2\lambda_w} \ln \frac{d_o}{d_i} + \frac{1}{h_s} \quad (38)$$

- (9) Carry out the heat duty, Φ , of the heat exchanger at present geometry. If Φ is around 15% greater than Φ_0 , then it means that the designed heat exchanger has a safety margin of 15% for the heat transfer. As an engineering design, usually 15 % extra heat transfer area (i.e., 15% redundancy) is acceptable for safe operation. Then the design procedure can be considered finished. If not, repeat steps (4)–(8), until the specified redundancy is satisfied.

For the rating mode, all the geometries are specified; the task is to evaluate the heat duty and pressure drop of heat exchanger, and steps (4)–(8) can be used for the rating mode.

5 Validations

As indicated above, one of the major contributions of the present paper is the replacement of the curves in Ref. [13] with

the equations shown in Sec. 2.3. Such a replacement was conducted with certain errors by reading the data from the graphs. Thus it is of crucial importance to validate whether such transformation can keep the unavoidable error within the acceptable range. As such a validation of the experimental data in Ref. [15] is adopted to validate the accuracy of the present method. Since the geometry parameters (see Table 1) and operation conditions are all known, rating calculation is performed to predict the over-all heat transfer coefficient and over-all pressure drop. The comparison between test data and calculation results is listed in Tables 2–4. It can be observed from the tables that the prediction accuracy of the present method is adequate for the engineering application.

6 Application of the Proposed Method

6.1 The Replacement of a Tube Core With SB by That With HB for a Common Shell. Because STHXsSB cause higher pressure drop or pump power, sometimes the heat transfer capacity of it has to be weakened with the increase in baffle spacing to meet the maximum allowable pressure drop. STHXsHB can reduce the pressure drop or pump power significantly and has a better comprehensive performance: At a fixed flow rate, the heat transfer coefficient per unit pressure drop or per unit pump power of STHXsHB is much higher than that of STHXsSB [12–15]. When a STHXHB is used to replace a STHXSB, if the reconstructed equipment has an equal pressure drop as the original heat exchanger, its heat transfer capacity must be larger than that of the original one; and if the reconstructed equipment has an equal heat transfer capacity, then it can definitely save pumping power. In the following presentation we will provide such engineering examples.

6.2 Replacement Examples. Four cases are provided to show the application of the present method, and the purpose of the design cases is to replace the original STHXSB with STHXHB. All the data for STHXSB come from heat exchangers in practical usage. In all the replacement design cases, the inner diameters of

Table 2 Validation of 20 deg helical baffled heat exchanger

	Experimental data		Calculation results		Deviation	
	Over-all heat transfer coefficient (W(m ² K) ⁻¹)	Over-all pressure drop for shell side (kPa)	Over-all heat transfer coefficient (W(m ² K) ⁻¹)	Over-all pressure drop for shell side (kPa)	Over-all heat transfer coefficient %	Over-all pressure drop for shell side %
1	134.4	1.29	165.9	0.96	23.4	-25.6
2	150.5	1.86	179.2	1.47	19.1	-21.0
3	175.7	4.32	202.1	3.65	15.0	-15.5
4	197.7	7.89	218.6	6.85	10.6	-13.2
5	201.6	10.9	228.3	9.69	13.2	-11.1

Table 3 Validation of 30 deg helical baffled heat exchanger

	Experimental data		Calculation results		Deviation	
	Over-all heat transfer coefficient (W(m ² K) ⁻¹)	Over-all pressure drop for shell side (kPa)	Over-all heat transfer coefficient (W(m ² K) ⁻¹)	Over-all pressure drop for shell side (kPa)	Over-all heat transfer coefficient %	Over-all pressure drop for shell side %
1	140.8	1.38	152.0	1.39	8.0	0.7
2	150.2	1.94	160.3	1.96	6.7	1.0
3	164.3	3.34	170.9	3.44	4.0	3.0
4	183.0	5.69	183.4	5.91	0.2	3.9
5	196.7	7.36	189.3	7.61	-3.8	3.4

Table 4 Validation of 40 deg helical baffled heat exchanger

	Experimental data		Calculation results		Deviation	
	Over-all heat transfer coefficient (W(m ² K) ⁻¹)	Over-all pressure drop for shell side (kPa)	Over-all heat transfer coefficient (W(m ² K) ⁻¹)	Over-all pressure drop for shell side (kPa)	Over-all heat transfer coefficient %	Over-all pressure drop for shell side %
1	280.7	20.0	337.3	23.15	20.2	15.8
2	298.5	25.4	353.4	28.65	17.7	12.8
3	305.8	32.0	366.5	35.27	19.8	10.2
4	324.3	41.3	384.2	44.3	18.5	7.3
5	339.8	49.3	398.9	53.9	17.4	9.3

shells and the tube layout pattern (excluding the tube effective length) remained unchanged to save the cost of manufacture modification.

6.2.1 Case 1. The original design data and comparison results are listed in Table 5. It shows that the comprehensive performance is greatly improved by using tube-core with 40 deg middle-overlapped helical baffles, and the pressure drop of STHXHB is 39% lower than that of original unit with 16% decrease in heat transfer area.

6.2.2 Case 2. Table 6 lists the original data and the comparison results. The usage of tube-core with 40 deg middle-overlapped helical baffles can reduce the over-all pressure drop by 46% compared to the original STHXSB, and the heat transfer area is 13% lower than that of original unit.

6.2.3 Case 3. The original data and comparison results are shown in Table 7. It shows that although the pressure drop of the heat exchanger with 40 deg middle-overlapped helical baffles is equivalent to that of the original STHXSB, the heat transfer area reduced by around 33% compared to the original STHXSB.

6.2.4 Case 4. In this case, 20 deg middle-overlapped helical baffles were adopted to replace the original unit (see Table 8, and the pressure drop in STHXHB is 33% lower than that of the original unit with 10% decrease in heat transfer area.

7 Conclusions

A method for the design and rating of STHXsHB is developed in the present paper based on the study results in Ref. [13] and the

Table 6 Design result for heat exchanger Case 2

Parameters	Unit	Original STHXSB	Designed STHXHB
Shell-side fluid		Water	Water
Tube side fluid		Water	Water
Shell-side flow rate	kg/h	133,242	133,242
Tube side flow rate	kg/h	25,278.6	25,278.6
Inlet/outlet temperature of shell side	°C	85/95	85/95
Inlet/outlet temperature of shell side	°C	210/160	210/160
d_o/d_i	mm	19×2	19×2
Tube arrangement		45 deg	45 deg
Tube effective length	mm	3000	2600
Tube No.		213	213
Inner diameter of shell	mm	500	500
Baffle spacing/helical pitch	mm	300	592.67
Over-all pressure drop for shell side	bar	0.225	0.12
Over-all heat transfer coefficient	W/m ² K	317.4	323.0
Heat transfer area	m ²	38.14	33.04

Table 5 Design result for heat exchanger Case 1

Parameters	Unit	Original STHXSB	Designed STHXHB
Shell-side fluid		Lean TEG	Lean TEG
Tube side fluid		Sea water	Sea water
Shell-side flow rate	kg/h	8195.6	8195.6
Tube side flow rate	kg/h	21,803.8	21,803.8
Inlet/outlet temperature of shell side	°C	81.1/41	81.1/41
Inlet/outlet temperature of shell side	°C	29.4/37.8	29.4/37.8
d_o/d_i	mm	19.05/15.75	19.05/15.75
Tube arrangement		30 deg	30 deg
Tube effective length	mm	5181	4445
Tube No.		90	90
Inner diameter of shell	mm	330	330
Baffle spacing/helical pitch	mm	184.9	391.4
Over-all pressure drop for shell side	bar	0.024	0.014
Over-all heat transfer coefficient	W/m ² K	406.0	471.3
Heat transfer area	m ²	28.58	23.92

Table 7 Design result for heat exchanger Case 3

Parameters	Unit	Original STHXSB	Designed STHXHB
Shell-side fluid		Mixture fluid	Mixture fluid
Tube side fluid		Mixture fluid	Mixture fluid
Shell-side flow rate	kg/h	177,328.4	177,328.4
Tube side flow rate	kg/h	35,470.3	35,470.3
Inlet/outlet temperature of shell side	°C	64.5/76	64.5/76
Inlet/outlet temperature of shell side	°C	210/160	210/160
d_o/d_i	mm	19×2	19×2
Tube arrangement		45 deg	45 deg
Tube effective length	mm	3000	2100
Tube No.		321	321
Inner diameter of shell	mm	600	600
Baffle spacing/helical pitch	mm	400	711.2
Over-all pressure drop for shell side	bar	0.13	0.12
Over-all heat transfer coefficient	W/m ² K	296.9	329.0
Heat transfer area	m ²	57.48	38.3

Table 8 Design result for heat exchanger Case 4

Parameters	Unit	Original STHXSB	Designed STHXHB
Shell-side fluid		320 conduction oil	320 conduction oil
Tube side fluid		Water	Water
Shell-side flow rate	kg/h	33,250.00	33,250.00
Tube side flow rate	kg/h	37,734.00	37,734.00
Inlet/outlet temperature of shell side	°C	55/40	55/40
Inlet/outlet temperature of tube side	°C	26/32	26/32
d_o/d_i	mm	10×1	10×1
Tube arrangement		30 deg	30 deg
Tube effective length	mm	2385	2150
Tube No.		440	440
Inner diameter of shell	mm	309	309
Baffle spacing/helical pitch	mm	250	160
Over-all pressure drop for shell side	bar	1.5	1.03
Over-all heat transfer coefficient	W/m ² K	477.8	607.0
Heat transfer area	m ²	32.97	31.09

Bell–Delaware method. The calculation procedure of the design method for STHXsHB is provided in detail, seemingly first in the public literature. One of the major contributions of the present paper is the replacement of those graphs in Ref. [13] by mathematical formulation with enough accuracy. From method validation and application examples, the following conclusions can be made.

1. The accuracy of the present method can meet the requirement of engineering design.
2. With an appropriate selection of geometric parameters the replacement of STHXsSB with STHXsHB usually can appreciably reduce shell-side pressure drop and reduce the heat transfer area at the same over-all heat transfer rate.

Acknowledgment

This work is supported by the National Fundamental Research Program of China (973 Program) (Grant No. 2007CB206902), the Key Project of Chinese Ministry of Education (Grant No. 306014), and the National Natural Science Foundation of China (Grant No. 50806057).

Nomenclature

Latin Symbols

- A_o = heat exchange area based on the outer diameter of tube, m²
 a = the ratio of distance between tube normal to the flow direction and the central tube pitch
 B = helical pitch for helical baffles, m
 b = the ratio of distance between tube in the flow direction and the central tube pitch
 c = specific heat, kJ kg K
 D_1 = inside diameter of the shell, m
 D_{ct} = the diameter of the circle through the centers of the tube located within the outermost tubes
 D_s = outside diameter of shell, m
 d_i = tube inner diameter, m
 d_o = outer diameter of tube, m
 ft = friction factor
 h = heat transfer coefficient, W(m² K)⁻¹
 k = over-all heat transfer coefficient, W(m² K)⁻¹

- k_c and k_e = friction factors for the sudden contraction or expansion effects when the tube side fluid flows into and out of the tubes
 l = characteristic dimension, m
 l_{ic} = the effective length of tube bundle, m
 l_{in} = the nonbaffled length of tube bundle, m
 l_{to} = the baffled length of tube bundle, m
 M = mass flux, kg/s
 N = tube number
 N_p = the number of tube passes
 N_t = number of tube rows
 Nu = Nusselt number
 n_r^1 = the number of tube rows on the center stream line within 1 cycle
 n_{rp} = the number of rows of tubes
 n_p = the number of baffles
 n_{pt} = the number of stealing strip pairs
 Δp = pressure drop, kPa
 Δp_{nozzle} = pressure drop in the inlet and outlet nozzles, kPa
 Δp_{i0}^1 = pressure drop cross the bundle per unit cycle without bypass flow, kPa
 Δp_{i0} = pressure drop cross the whole bundle zone with bypass flow, kPa
 Δp_{in} = pressure drop in inlet and outlet zone, kPa
 Re = Reynolds number
 S_{ss} = bundle-to-tube cross-flow bypass area per baffle, m²
 S_{2z} = the cross-flow area at the shell centerline, m²
 S_p = the thickness of baffle, mm
 S_{it} = distance between two tube outside surfaces, m
 t = temperature, °C
 Δt_m = logarithmic mean temperature difference, K
 t_i = tube pitch, mm
 v_{nozzle} = fluid velocity in nozzles, m s⁻¹
 Y_i and Z_i = correction factor for heat transfer coefficient and pressure drop, respectively

Greek Symbols

- β = helix angle
 Φ = heat duty, W
 λ = conductivity factor of tube wall, W(m K)⁻¹
 λ_{22} = the friction factor of ideal cross-flow through tube bundle
 ρ = density of shell-side fluid, kg m⁻³
 η = dynamics viscosity of shell-side fluid, Pa s
 ξ = nozzle pressure drop coefficient

Subscripts

- in = inlet
lm = laminar
out = outlet
s = shell side
t = tube side
turb = turbulence
w = wall

References

- [1] Master, B. I., Chunangad, K. S., and Pushpanathan, V., 2003, "Fouling Mitigation Using Helixchanger Heat Exchangers," *Proceedings of the ECI Conference on Heat Exchanger Fouling and Cleaning: Fundamentals and Applications*, Santa Fe, NM, May 18–22, pp. 317–322.
- [2] Bell, K. J., 1981, "Delaware Method for Shell Side Design," *Heat Exchangers Thermal Hydraulic Fundamentals and Design*, S. Kakac, A. E. Bergles, and F. Mayinger, eds., Taylor & Francis, Washington, DC.
- [3] Bell, K. J., 1986, "Delaware Method of Shell Side Design," *Heat Exchanger Sourcebook*, J. W. Pallen, ed., Hemisphere, Washington, DC.
- [4] Bell, K. J., 1988, "Delaware Method of Shell-Side Design," *Heat Transfer Equipment Design*, R. K. Shah, E. C. Sunnarao, and R. A. Mashelkar, eds., Taylor & Francis, New York.
- [5] Bell, K. J., 2004, "Heat Exchanger Design for the Process Industries," ASME

- J. Heat Transfer, **126**(6), pp. 877–885.
- [6] Schlünder, E. U., ed., 1983, *Heat Exchanger Design Handbook*, Vol. 3, Hemisphere, Washington, DC.
- [7] Mukherjee, R., 1992, "Use Double-Segmental Baffles in the Shell-and-Tube Heat Exchangers," Chem. Eng. Prog., **88**, pp. 47–52.
- [8] Saffar-Avval, M., and Damangir, E., 1995, "A General Correlation for Determining Optimum Baffle Spacing for All Types of Shell and Tube Exchangers," Int. J. Heat Mass Transfer, **38**(13), pp. 2501–2506.
- [9] Li, H. D., and Kottke, V., 1998, "Effect of Baffle Spacing on Pressure Drop and Local Heat Transfer in Shell-and-Tube Heat Exchangers for Staggered Tube Arrangement," Int. J. Heat Mass Transfer, **41**(10), pp. 1303–1311.
- [10] Stehlik, P., and Wadekar, V. V., 2002, "Different Strategies to Improve Industrial Heat Exchange," Heat Transfer Eng., **23**(6), pp. 36–48.
- [11] Khalifeh Soltan, B., Saffar-Avval, M., and Damangir, E., 2004, "Minimization of Capital and Operating Costs of Shell and Tube Condensers Using Optimum Baffle Spacing," Appl. Therm. Eng., **24**(17–18), pp. 2801–2810.
- [12] Lutcha, J., and Nemicansky, J., 1990, "Performance Improvement of Tubular Heat Exchangers by Helical Baffles," Trans. Inst. Chem. Eng., Part A, **68**, pp. 263–270.
- [13] Stehlik, P., Nemicansky, J., and Kral, D., 1994, "Comparison of Correction Factors for Shell-and-Tube Heat Exchangers With Segmental or Helical Baffles," Heat Transfer Eng., **15**(1), pp. 55–65.
- [14] Kral, D., Stelick, P., Van Der Ploeg, H. J., and Masster, B. I., 1996, "Helical Baffles in Shell-and-Tube Heat Exchangers, Part One: Experimental Verification," Heat Transfer Eng., **17**(1), pp. 93–101.
- [15] Zhang, J. F., Li, B., Huang, W. J., Lei, Y. G., He, Y.-L., and Tao, W. Q., 2009, "Experimental Performance Comparison of Shell Side Heat Transfer for Shell-and-Tube Heat Exchangers With Middle-Overlapped Helical Baffles and Segmental Baffles," Chem. Eng. Sci., **64**, pp. 1643–1653.
- [16] Shuli, W., 2002, "Hydrodynamic Studies on Heat Exchangers With Helical Baffles," Heat Transfer Eng., **23**(3), pp. 43–49.
- [17] Zhnegguo, Z., Tao, X., and Xiaoming, F., 2004, "Experimental Study on Heat Transfer Enhancement of a Helically Baffled Heat Exchanger Combined With Three-Dimensional Finned Tubes," Appl. Therm. Eng., **24**(14–15), pp. 2293–2300.
- [18] Peng, B., Wang, Q. W., Zhang, C., Xie, G. N., Luo, L. Q., Chen, Q. Y., and Zeng, M., 2007, "An Experimental Study of Shell-and-Tube Heat Exchangers With Continuous Helical Baffles," ASME J. Heat Transfer, **129**, pp. 1425–1431.
- [19] Lei, Y. G., He, Y. L., Chu, P., and Li, R., 2008, "Design and Optimization of Heat Exchangers With Helical Baffles," Chem. Eng. Sci., **63**, pp. 4386–4395.
- [20] Patankar, S. V., and Spalding, D. B., 1974, "A Calculation Procedure for the Transient and Steady State Behavior of Shell-and-Tube Heat Exchanger," *Heat Exchanger Design and Theory Source Book*, N. F. Afgan and E. U. Schlunder, eds., McGraw-Hill, New York.
- [21] Butterworth, D., 1978, "A Model for Heat Transfer During Three-Dimensional Flow in Tube Bundles," Sixth International Heat Transfer Conference, Toronto, Canada, Paper No. HX-6.
- [22] Sha, W. T., 1980, "An Overview on Rod-Bundle Thermal-Hydraulic Analysis," Nucl. Eng. Des., **62**, pp. 1–24.
- [23] Sha, W. T., Yang, C. I., Kao, T. T., and Cho, S. M., 1982, "Multi-Dimensional Numerical Modeling of Heat Exchangers," ASME J. Heat Transfer, **104**, pp. 417–425.
- [24] Prithiviraj, M., and Andrews, M. J., 1998, "Three-Dimensional Numerical Simulation of Shell-and-Tube Heat Exchanger. Part I: Foundation and Fluid Mechanics," Numer. Heat Transfer, Part A, **33**, pp. 799–816.
- [25] Prithiviraj, M., and Andrews, M. J., 1998, "Three-Dimensional Numerical Simulation of Shell-and-Tube Heat Exchanger. Part II: Heat Transfer," Numer. Heat Transfer, Part A, **33**, pp. 817–828.
- [26] Prithiviraj, M., and Andrews, M. J., 1999, "Comparison of a Three-Dimensional Numerical Model With Existing Methods for Prediction of Flow in Shell-and-Tube Heat Exchangers," Heat Transfer Eng., **20**(2), pp. 15–19.
- [27] Deng, B., 2003, "Experimental and Numerical Study of Flow and Heat Transfer in the Shell Side of Heat Exchangers," Ph.D. thesis, Xi'an Jiaotong University, Xi'an, China.
- [28] Andrews, M. J., and Master, B. I., 1999, "3-D Modeling of the ABB Lummus Heat Transfer Helixchanger Using CFD," International Conference on Compact Heat Exchangers, Banff, Canada.
- [29] Andrews, M. J., and Master, B. I., 2005, "Three-Dimensional Modeling of a Helixchanger[®] Heat Exchanger Using CFD," Heat Transfer Eng., **26**, pp. 22–31.
- [30] Schröder, K., and Gelbe, H., 1999, "Two- and Three-Dimensional CFD-Simulation of Flow-Induced Vibration Excitation in Tube Bundles," Chem. Eng. Process., **38**, pp. 621–629.
- [31] Mohr, U., and Gelbe, H., 2000, "Velocity Distribution and Vibration Excitation in Tube Bundle Heat Exchangers," Int. J. Therm. Sci., **39**, pp. 414–421.
- [32] Philpott, C., and Deans, J., 2004, "The Enhancement of Steam Condensation Heat Transfer in a Horizontal Shell and Tube Condenser by Addition of Ammonia," Int. J. Heat Mass Transfer, **47**, pp. 3683–3693.
- [33] Karlsson, T., and Vamling, L., 2005, "Flow Fields in Shell-and-Tube Condensers: Comparison of a Pure Refrigerant and a Binary Mixture," Int. J. Refrig., **28**, pp. 706–713.
- [34] Lee, S. H., and Hur, N., 2007, "Numerical Analysis of the Fluid Flow and Heat Transfer in a Shell and Tube Heat Exchanger," *Proceedings of the First Asian Symposium on Computational Heat Transfer and Fluid Flow*, Xi'an, China.
- [35] Shen, R. J., Feng, X., and Gao, X. D., 2004, "Mathematical Model and Numerical Simulation of Helical Baffles Heat Exchanger," J. Enhanced Heat Transfer, **11**, pp. 461–466.
- [36] Lei, Y. G., He, Y. L., Li, R., and Gao, Y. F., 2008, "Effects of Baffle Inclination Angle on Flow and Heat Transfer of a Heat Exchanger With Helical Baffles," Chem. Eng. Process., **47**(12), pp. 2336–2345.
- [37] Jafari Nasr, M. R., and Shafeghat, A., 2008, "Fluid Flow Analysis and Extension of Rapid Design Algorithm for Helical Baffle Heat Exchangers," Appl. Therm. Eng., **28**, pp. 1324–1332.
- [38] Zhang, J. F., He, Y. L., and Tao, W. Q., 2009, "3D Numerical Simulation on Shell-and-Tube Heat Exchangers With Middle-Overlapped Helical Baffles and Continuous Baffles—Part I: Numerical Model and Results of Whole Heat Exchanger With Middle-Overlapped Helical Baffles," Int. J. Heat Mass Transfer, **52**(23–24), pp. 5371–5380.
- [39] Zhang, J. F., He, Y. L., and Tao, W. Q., 2009, "3D Numerical Simulation on Shell-and-Tube Heat Exchangers With Middle-Overlapped Helical Baffles and Continuous Baffles—Part II: Simulation Results of Periodic Model and Comparison Between Continuous and Noncontinuous Helical Baffles," Int. J. Heat Mass Transfer, **52**(23–24), pp. 5381–5389.
- [40] Kern, D. Q., 1950, *Process Heat Transfer*, McGraw-Hill, New York.
- [41] Tinker, T., 1958, "Shell-Side Characteristics of Shell-and-Tube Heat Exchangers: A Simplified Rating System for Commercial Heat Exchangers," Trans. ASME, **80**, pp. 36–52.
- [42] Palen, J. W., and Taborek, J., 1969, "Solution of Shell Side Flow Pressure Drop and Heat Transfer by Stream Analysis Method," Chem. Eng. Prog., Symp. Ser., **65**(93), pp. 53–63.
- [43] Reppich, M., and Zagermann, S., 1995, "A New Design Method for Segmentally Baffled Heat Exchangers," Comput. Chem. Eng., **19**, pp. S137–S142.
- [44] Serna, M., and Jimenez, A., 2004, "An Efficient Method for the Design of Shell and Tube Heat Exchangers," Heat Transfer Eng., **25**(2), pp. 5–16.
- [45] Kara, Y. A., and Güraras, Ö., 2004, "A Computer Program for Designing of Shell-and-Tube Heat Exchangers," Appl. Therm. Eng., **24**(13), pp. 1797–1805.
- [46] Del Col, D., Muzzolon, A., Piubello, P., and Rosetto, L., 2005, "Measurement and Prediction of Evaporator Shell-Side Pressure Drop," Int. J. Refrig., **28**, pp. 320–330.
- [47] Ayub, Z. H., 2005, "A New Chart Method for Evaluating Single-Phase Shell Side Heat Transfer Coefficient in a Single Segmental Shell and Tube Heat Exchanger," Appl. Therm. Eng., **25**(14–15), pp. 2412–2420.
- [48] Selbas, R., Önder, K., and Reppich, M., 2006, "A New Design Approach for Shell-and-Tube Heat Exchangers Using Genetic Algorithms From Economic Point of View," Chem. Eng. Process., **45**(4), pp. 268–275.
- [49] Caputo, A. C., Pelagagge, P. M., and Salini, P., 2008, "Heat Exchanger Design Based on Economic Optimization," Appl. Therm. Eng., **28**(10), pp. 1151–1159.
- [50] Fesanghary, M., Damangir, E., and Soleimani, I., 2009, "Design Optimization of Shell and Tube Heat Exchangers Using Global Sensitivity Analysis and Harmony Search Algorithm," Appl. Therm. Eng., **29**(5–6), pp. 1026–1031.
- [51] Ponce-Ortega, J., Serna-González, M., and Jiménez-Gutiérrez, A., 2009, "Use of Genetic Algorithms for the Optimal Design of Shell-and-Tube Heat Exchangers," Appl. Therm. Eng., **29**(2–3), pp. 203–209.
- [52] Schlünder, E. U., ed., 1983, *Heat Exchanger Design Handbook*, Vol. 2, Hemisphere, Washington, DC.
- [53] Gaddis, E. S., and Gnielinski, V., 1997, "Pressure Drop on the Shell Side of Shell-and-Tube Heat Exchangers With Segmental Baffles," Chem. Eng. Process., **36**(2), pp. 149–159.
- [54] Kuppan, T., 2000, *Heat Exchanger Design Handbook*, Marcel Dekker, New York.
- [55] Li, B., 2007, "Numerical Simulation and Experimental Study on Heat Transfer Enhancement in Air and Oil Heat Transfer Equipment," Ph.D. thesis, Xi'an Jiaotong University, Xi'an, China.
- [56] Incropera, F. P., and DeWitt, D. P., 2002, *Heat and Mass Transfer*, 5th ed., Wiley, New York.
- [57] Yang, S. M., and Tao, W. Q., 1998, *Heat Transfer*, 3rd ed., High Education, Beijing, China.
- [58] Gnielinski, V., 1976, "New Equations for Heat and Mass Transfer in Turbulent Pipe and Channel Flows," Int. Chem. Eng., **16**, pp. 359–368.